

Influence of incommensurate dynamic charge-density wave scattering on the line shape of superconducting high- T_c cuprates

G. Seibold[†] and M. Grilli^{*}

[†] Institut für Physik, BTU Cottbus, PBox 101344, 03013 Cottbus, Germany

^{*} Istituto Nazionale di Fisica della Materia e Dipartimento di Fisica, Università di Roma “La Sapienza”, Piazzale A. Moro 2, 00185 Roma, Italy

We show that the spectral lineshape of superconducting $\text{La}_{2-x}\text{Sr}_x\text{CuO}_4$ (LSCO) and $\text{Bi}_2\text{Sr}_2\text{CaCu}_2\text{O}_{8+\delta}$ (Bi2212) can be well described by the coupling of the charge carriers to collective incommensurate charge-density wave (CDW) excitations. Our results imply that besides antiferromagnetic (AF) fluctuations also low-energy CDW modes can contribute to the observed dip-hump structure in the Bi2212 photoemission spectra. In case of underdoped LSCO we propose a possible interpretation of ARPES data in terms of a grid pattern of fluctuating stripes where the charge and spin scattering directions deviate by $\alpha = \pi/4$. Within this scenario we find that the spectral intensity along $(0, 0) \rightarrow (\pi, \pi)$ is strongly suppressed consistent with recent photoemission experiments. In addition the incommensurate charge-density wave scattering leads to a significant broadening of the quasiparticle-peak around $(\pi, 0)$.

I. INTRODUCTION

There is an increasing experimental evidence [1,2] that the peculiar properties of the superconducting cuprates, both in the normal and the superconducting phase are related to the occurrence of a Quantum Critical Point (QCP) located near (slightly above) the optimal doping. These evidences corroborate the consensus that quantum criticality related to some “exotic” [3] or more traditional [4–8] type of ordering is at work in these systems. Accordingly the phase diagram of the cuprates is naturally partitioned in a (nearly) ordered, a quantum critical, and a quantum disordered region naturally corresponding to the under-, optimally, and over-doped regions of the phase diagram of the cuprates respectively. In this framework a key open issue is to determine the type of ordering which is established (at least in a local and slowly dynamical sense) in the underdoped phase of the cuprates. While the direct detection of the exotic order is more difficult and elusive, it is quite natural that the spin and charge fluctuations associated to the more traditional proposals [4–7] affect in a rather apparent way the physical properties. Especially one would expect that the modification of the electronic structure due to dynamical spin- or charge scattering should be observable in angle-resolved photoemission spectroscopy (ARPES). In fact, ARPES data of high- T_c $\text{Bi}_2\text{Sr}_2\text{CaCu}_2\text{O}_{8+\delta}$ (Bi2212) compounds show several specific features in the superconducting state which can be interpreted in terms of a coupling of the electrons to a collective mode [9]. Below T_c , these spectra are characterized by an unusual lineshape around $(\pi, 0)$ (M-point) which consists of a sharp peak at low energy followed by a hump at higher energies. Both features are separated by a dip. In addition the sharp peak persists at low energy over a large region in k -space whereas the hump correlates well with the underlying normal state dispersion [10]. Since the

energy difference between dip and peak position is similar to the energy of the (π, π) resonance observed in inelastic neutron scattering [11] it has been suggested that the mode responsible for the ARPES features corresponds to collective spin fluctuations [12]. Although this proposal is quite appealing one needs to understand by which mechanism the substantial spin fluctuations can be sustained in optimally and overdoped materials. In fact, since doping rapidly disrupts the antiferromagnetic (AF) order and with the occurrence of an AF-QCP in the very underdoped region where the Neél temperature vanishes, spin scattering should be a minor effect at large dopings. This difficulty can be overcome by considering the (traditional) ordering in the underdoped phase to be driven by the charge. Then the occurrence of (a local and possibly slowly dynamical) charge ordering is naturally accompanied by substantial spin fluctuations since the spin coupling resurges in the hole-depleted regions. This strong spin and charge coupling is also an effective mechanism driving the weak charge modulation around the second-order quantum transition to strongly anharmonic charge (and spin) *stripes* in the deeply underdoped materials. The relevant role of charge ordering has a solid experimental support at least in some classes of cuprates. First evidence for incommensurate stripe structures in the high- T_c compounds was given by neutron scattering experiments [13] in Nd-doped lanthanum cuprate. Here the Low-Temperature Tetragonal (LTT) lattice structure is suitable to effectively pin the charge stripes giving rise to static stripe ordering so that both magnetic and charge-order peaks become detectable. However, also in Nd-free materials including the YBCO compounds where the magnetic incommensurate peak has been observed [14,15] the simultaneous occurrence of charge order has been claimed in Ref. [16] and from NQR measurements in Refs. [17–20]. Moreover, it has been argued [1] that the QCP can be deduced from the incommensurate neu-

tron peak intensity which vanishes in the slightly over-doped regime $x \approx 0.19$. This coincides surprisingly well with experiments in $\text{La}_{2-x}\text{Sr}_x\text{CuO}_4$ (LSCO) compounds where superconductivity has been suppressed by pulsed magnetic fields [2] showing an underlying metal-insulator transition at about the same critical doping. Recent photoemission experiments [21–23] on superconducting underdoped $\text{La}_{2-x}\text{Sr}_x\text{CuO}_4$ (LSCO) have also revealed a broad quasiparticle peak (QP) around the $(\pi, 0)$ point. On the other hand no QP can be identified along the $(0, 0) \rightarrow (\pi, \pi)$ direction in contrast to the Bi2212 compound where along the diagonals a clear Fermi surface crossing has been observed. Exact diagonalization studies of the t-t'-t"-J model with an additional phenomenological stripe potential [24] have demonstrated that these features may be due to the coupling of the holes to vertical charged (static) stripes.

In the present paper we want to focus on the dynamic aspect of incommensurate charge-density wave (CDW) scattering within the framework of a QCP scenario. In this context we discuss the differences between the photoemission spectra of Bi2212 and LSCO respectively. Especially we show that the different features can be explained by the assumption that in Bi2212 the charge carriers couple to an incommensurate CDW oriented along the $(1, 0)$ – and $(0, 1)$ – directions whereas in LSCO the dynamic CDW scattering is along the diagonals. The results presented below supplement considerations of Ref. [25] where we have shown that a two-dimensional 'eggbox-type' charge-pattern can reproduce the essential features of the normal state Bi2212 Fermi surface, namely the reduction of spectral weight around the M-points associated with the opening of a pseudo-gap in these regions of k-space. Here we extend our considerations to the case of LSCO assuming that the k-dependence of the electron self-energy is an essential ingredient in the description of ARPES data.

We note that in a recent paper [26] Eschrig and Norman have analyzed ARPES data within a model of electrons interacting with a magnetic resonance using a similar approach than in the present paper. Comparing their results with those reported below one can see that AF and CDW scattering have similar effects on the electronic states around the M-points and the similarity between our results and those in Ref. [26] provides a support to the idea that spin and charge fluctuations coexist and cooperate in determining the spectral properties.

After having introduced the formalism in Sec. II we will present in Sec. III the analysis of ARPES spectra for both LSCO and Bi2212 materials. We finally conclude our discussion in Sec. IV.

II. FORMALISM

We consider a system of superconducting electrons exposed to an effective action

$$S = -\lambda^2 \sum_q \int_0^\beta d\tau_1 \int_0^\beta d\tau_2 \chi_q(\tau_1 - \tau_2) \rho_q(\tau_1) \rho_{-q}(\tau_2) \quad (1)$$

describing dynamical incommensurate CDW fluctuations. Using Nambu-Gorkov notation the unperturbed Matsubara Greens function matrix $\underline{\underline{G}}$ is given by

$$G_{11}^0(k, i\omega) = \frac{u_k^2}{i\omega - E_k} + \frac{v_k^2}{i\omega + E_k} \quad (2)$$

$$G_{22}^0(k, i\omega) = \frac{v_k^2}{i\omega - E_k} + \frac{u_k^2}{i\omega + E_k} \quad (3)$$

$$G_{12}^0(k, i\omega) = G_{21}^0(k, i\omega) = -u_k v_k \left[\frac{1}{i\omega - E_k} - \frac{1}{i\omega + E_k} \right] \quad (4)$$

where the BCS coherence factors are defined as $u_k^2 = \frac{1}{2}(1 + \frac{\epsilon_k - \mu}{E_k})$ and $v_k^2 = \frac{1}{2}(1 + \frac{\epsilon_k + \mu}{E_k})$ respectively. The leading order one-loop contribution to the self-energy reads as

$$\underline{\underline{\Sigma}}(k, i\omega) = -\frac{\lambda^2}{\beta} \sum_{q, ip} \chi_q(ip) \tau_z \underline{\underline{G}}^0(k - q, i\omega - ip) \tau_z \quad (5)$$

which in turn allows for the calculation of $\underline{\underline{G}}$ via

$$\underline{\underline{G}} = \underline{\underline{G}}^0 + \underline{\underline{G}}^0 \underline{\underline{\Sigma}} \underline{\underline{G}}. \quad (6)$$

It should be mentioned that the self-energy eq. (5) differs from the analogous expression for the coupling to spin-fluctuations by the τ_z Pauli matrices. Finally the spectral function can be extracted from $A_k(\omega) = \text{Im}G_{11}(k, \omega)$.

Note that our approach differs from the standard Elisahberg treatment by the fact that already the unperturbed system displays coherent superconducting order. Since the incommensurate CDW fluctuations have been shown to be strongly attractive in the d-wave channel [7] the idea is to incorporate this feature already on the zeroth order level by a frequency independent d-wave order parameter. Thus the self-energy is gapped by $\underline{\underline{G}}^0$, however, for our present considerations this approximation is sufficient since we are interested in line shape phenomena occurring at energies $\omega \gg \Delta^{SC}$.

III. RESULTS

In order to simplify the calculations we consider a Kampf-Schrieffer-type model susceptibility [27] which is factorized into an ω - and q -dependent part, i.e.

$$\chi_q(i\omega) = W(i\omega) J(\mathbf{q}) \quad (7)$$

where $W(\omega) = -\int d\nu g(\nu) 2\nu / (\omega^2 + \nu^2)$ is some distribution of dispersionless propagating bosons and

$$J(\mathbf{q}) = \frac{\mathcal{N}}{4} \sum_{\pm q_x^c; \pm q_y^c} \frac{\Gamma}{\Gamma^2 + 2 - \cos(q_x - q_x^c) - \cos(q_y - q_y^c)}. \quad (8)$$

\mathcal{N} is a suitable normalization factor introduced to keep the total scattering strength constant while varying Γ . The above susceptibility contains the charge-charge correlations which are enhanced at the four equivalent critical wave vectors $(\pm q_x^c, \pm q_y^c)$. As we will show below the static limit $g(\nu) = \delta(\nu)$ together with an infinite charge-charge correlation length $\Gamma \rightarrow 0$ allows one to relate the coupling parameter λ to the parameter set of the Hubbard-Holstein model with long-range Coulomb interaction by following the approach in Ref. [25]. Concerning the normal state dispersion we use a tight-binding fit to normal state ARPES data [28,29] including the hopping between first, second and third nearest neighbors, i.e. $\epsilon_k = t(\cos(k_x) + \cos(k_y))/2 + t' \cos(k_x) \cos(k_y) + t''(\cos(2k_x) + \cos(2k_y))/2$. For Bi2212 we take $t = -0.59$, $t' = 0.164$, $t'' = -0.052$ and for LSCO $t = -0.35$, $t' = 0.042$, $t'' = -0.028$. The BCS gap is assumed to be d-wave symmetry $\Delta_{SC}(\mathbf{k}) = \Delta_0(\cos(k_x) - \cos(k_y))$ where $\Delta_0(\text{Bi2212}) = 32\text{meV}$ and $\Delta_0(\text{LSCO}) = 10\text{meV}$ respectively.

A. $\text{Bi}_2\text{Sr}_2\text{CaCu}_2\text{O}_{8+\delta}$

In Ref. [25] we have already demonstrated that a static two-dimensional eggbox-type charge modulation with \mathbf{q}_c oriented along the vertical directions can account for the basic Fermi surface (FS) features in the optimally and underdoped Bi2212 compounds. Here we supplement these considerations by a detailed analysis of the photoemission lineshape in the superconducting state. Concerning the frequency dependent part of the susceptibility we restrict ourselves to the simplest case of a single energy excitation, i.e. we choose $g(\nu) = \delta(\nu - \omega_0)$.

The coupling of electrons with a dispersionless bosonic mode is a well known subject in solid state theory and has been intensively investigated in [30]. In the present context the new feature is a) the inclusion of superconductivity and b) the role of a strongly \mathbf{q} -dependent coupling between electrons and the incommensurate CDW mode.

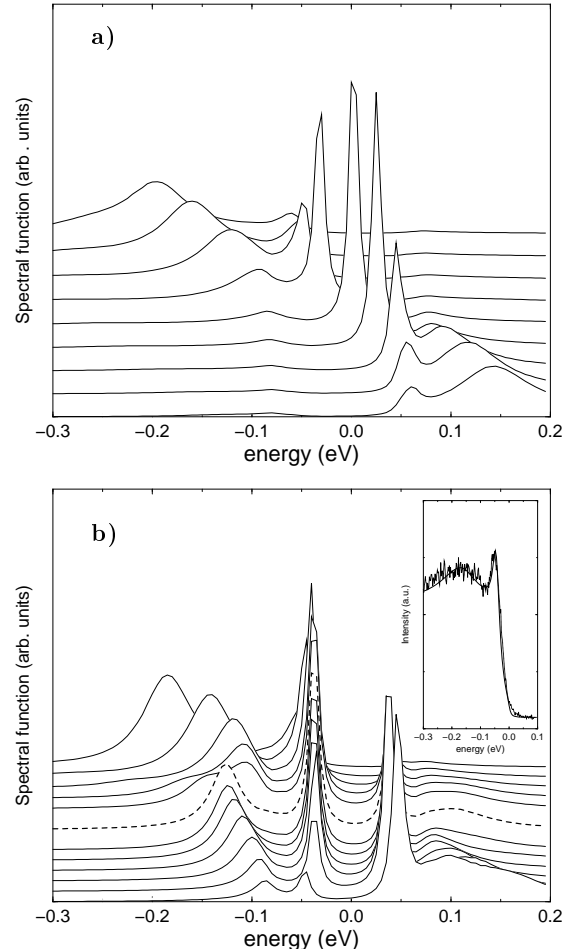


FIG. 1. Spectral functions for states from (top to bottom) (a) $(0.15\pi, 0.36\pi) \rightarrow (0.5\pi, 0.36\pi)$ and (b) $(0.5\pi, 0) \rightarrow (\pi, 0) \rightarrow (\pi, 0.3\pi)$. The dashed line corresponds to the M-point. Parameters: $\omega_0 = 40\text{meV}$, $\lambda = 10\text{meV}$, $\Gamma = 0.1$, $|q_c| = \pi/4$. Temperature $T = 40\text{K}$. Inset: Spectral function at $(\pi, 0)$ in comparison with experimental data points for an underdoped sample with $T_c = 70\text{K}$ measured at 40K . A step-like function has been added in order to incorporate the background. Parameters: $\omega_0 = 70\text{meV}$, $\lambda = 55\text{meV}$, $\Gamma = 0.5$, $|q_c| = \pi/3$.

In Figs. 1 (a) and (b) we show the spectral function for two “vertical” cuts, one through the order parameter node at the Fermi energy $(0.2\pi, 0.36\pi) \rightarrow (0.5\pi, 0.36\pi)$ and the other for a cut from $(0.5\pi, 0) \rightarrow (\pi, 0) \rightarrow (\pi, 0.3\pi)$. Parameters have been chosen in approximate analogy to the ones used in [26].

The effect of the weight function $J(\mathbf{q})$ is to strongly reduce the scattering along the diagonals since the states (\mathbf{k}, ω) and $(\mathbf{k} + \mathbf{q}_c, \omega - \omega_0)$ which are coupled via the CDW fluctuations are very different in energy. As a consequence the quasiparticles are poorly scattered by the charge collective modes. Therefore the hump feature is suppressed near the node and one observes a single dis-

persive quasiparticle peak at the Fermi energy. Scanning away from the node towards $(0.2\pi, 0.36\pi)$ (Fig. 1a) the low energy peak rapidly loses weight in favor of the hump feature at higher binding energy. This latter broad peak arises because moving away from the Fermi surface the quasiparticles have enough energy to excite charge fluctuations with $\mathbf{q} \sim \mathbf{q}_c$ and are strongly damped. In this region of the momentum space the lower-energy narrow peak progressively acquires the character of the collective mode while the hump becomes dispersive as a remnant of the underlying quasiparticle band. The behavior of the spectral density along this first cut is rather similar to the case of electrons coupled to a dispersionless phonon [30]. In this latter case, however, the phonons are coupled to the quasiparticles for any momentum transfer leading to broad incoherent features at high energy even for quasiparticles on the Fermi surface. On the contrary, in the present case, the scattering between the quasiparticles near the node is severely suppressed by the factor $J(\mathbf{q})$ and the incoherent hump is nearly absent when the quasiparticle is close to the Fermi surface (i.e. near the node at $(0.36\pi, 0.36\pi)$). The switching of the underlying quasiparticle from the low-energy peak to the hump structure leads to a break in the dispersion. This break of the dispersion is also observed experimentally [31] however, only for momentum scans far from the node. We want to note that the discrepancy of the break-location is a consequence of our approximation of a factorized susceptibility and should be less pronounced in a more realistic model. An additional possible difficulty for the present scheme is that the quasiparticles near the node are only weakly scattered and therefore, according to the standard Landau theory of Fermi liquids, they should have a damping rate proportional to T^2 and to (binding energy) 2 . This Fermi-liquid behavior is violated in recent experiments carried above and below T_c [32]. However, these experiments were not carried out at very low temperatures, where a fair comparison can be done with our $T = 0$ analysis, and where heat-transport experiments report a rather standard Fermi-liquid behavior of the quasiparticles [33] (thereby supporting our finding of well-defined quasiparticles near the nodes). This issue obviously deserves further experimental and theoretical investigation.

Fig. 1b displays the spectral functions for states from $(0.5\pi, 0) \rightarrow (\pi, 0) \rightarrow (\pi, 0.3\pi)$. The appearance of states with positive energy is due to coherence effects related to the finite superconducting gap in this region of momentum space. Since the M-point defines the 'hot' region for incommensurate CDW scattering the superconducting states couple strongly to the CDW mode and as a result the spectrum (dashed line) is characterized by the peak-dip-hump feature as observed in ARPES. For a suitable choice of parameters we can obtain a quite satisfactory fit of our curve with experimental data from photoemission experiments (see inset of Fig. 1b).

Note that the structure of the hump feature is mainly determined by the charge-charge correlation function $J(\mathbf{q})$. From our fit to the experimental data we can therefore deduce that in Bi2212 the underlying CDW fluctuations are rather short-ranged i.e. the stripe correlations extend over 2-3 unit cells only. The spectra for the scan $(0.5\pi, 0) \rightarrow (\pi, 0)$ show an interesting feature which is also observed in ARPES (see e.g. [12], Fig. 3): The sharp peak at low energies is essentially non-dispersive whereas the hump exhibits a maximum binding energy ω_{max} . For energies large than ω_{max} the hump dispersion again corresponds to the underlying (normal state) band structure. The maximum in the hump dispersion is due to the reduced scattering efficiency (determined by $J(\mathbf{q})$) when moving away from the M-point. Since along $(\pi, 0) \rightarrow (0, 0)$ the underlying dispersion ϵ_k initially is rather flat this leads to a shift of the hump to lower energies. With k_x becoming smaller the increasing band dispersion then starts to determine the dispersion of the hump which accordingly shifts to higher binding energies.

Scanning from M towards (π, π) the hump moves to lower energies and loses weight again in agreement with photoemission experiments [12,31]. We want to point out that our result for the spectral functions in Fig. 1 are rather similar to analogous results of Ref. [26] where the coupling of electrons to an AF mode has been considered. Indeed for both AF and incommensurate CDW scattering the states around $(\pi, 0)$ are the 'hot points', i.e. are most strongly affected by the scattering.

This indicates that in the real systems the spin and the charge fluctuations may well coexist and cooperate in determining the spectral properties. Of course for a quantitative comparison with experiments one should include both scattering channels. On the contrary, since we aim to explore and underline the role of charge fluctuations only, in the inset of Fig. 1(b) we fitted for an illustrative purpose, the experimental data with the charge channel only.

B. $\text{La}_{2-x}\text{Sr}_x\text{CuO}_4$

In underdoped $\text{La}_{2-x}\text{Sr}_x\text{CuO}_4$ the incommensurate magnetic fluctuations display a four-fold pattern around (π, π) . For the Nd-doped lanthanum cuprate it has been argued [34] that this may be related to two types of twin domains, each with a single stripe orientation suitably pinned by the underlying LTT lattice structure. However, this kind of argument no longer holds in case of underdoped LSCO where both the (tetragonal) a- and b- axes are at about 45° with respect to the CuO_6 tilt direction. Moreover it has been demonstrated in Refs. [35,36] that the positions of the elastic magnetic peaks in $\text{La}_{1.88}\text{Sr}_{0.12}\text{CuO}_4$ and excess-oxygen doped $\text{La}_2\text{CuO}_{4+y}$ are shifted off of the high-symmetry Cu-O-Cu directions by a tilt angle of $\Theta \approx 3^\circ$. For a one-dimensional stripe

model this would correspond to one kink every ~ 19 Cu sites on the charge domain wall. However, as explicitly stated in Ref. [36] a grid pattern of orthogonal stripes oriented along the two orthorombic directions adequately describes the data as well.

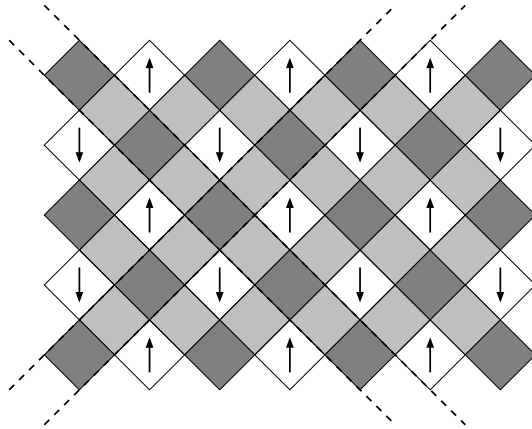


FIG. 2. Sketch of the two-dimensional charge- and spin modulation which is consistent with the AF peak incommensurability of LSCO. The pattern can be constructed from charge stripes running along the diagonal directions as indicated by the dashed lines. The crossing of two stripes leads to regions with high charge density (dark squares) whereas the residual segments of the stripes have intermediate charge (lightly shaded squares). The white squares illustrate the charge depleted areas with maximal spin density while the arrows indicate the sign of the AF order parameter.

In the following we therefore examine the consequences of this kind of two-dimensional dynamic stripe fluctuations on the electronic structure of LSCO and compare with photoemission experiments. Denoting the two orthogonal charge scattering vectors (which for simplicity we assume to have equal magnitude) by $\mathbf{q}_c^\pm = q_c(1, \pm 1)$ the charge modulation can be written as $\rho(\mathbf{R}) \sim \cos(q_c x) \cos(q_c y)$. Fig. 2 shows a sketch of the corresponding charge pattern which can be thought of an array of stripes running along the $(1, 1)$ and $(1, -1)$ directions respectively. Although our calculations are restricted on the charge channel we want to note that the corresponding pattern of the spin order can be constructed by assuming a sign change of the AF order parameter upon crossing the stripes perpendicular to their orientation. This antiphase correlation between the spins across a charge stripe makes easier the transversal delocalization of the charges in the stripes and therefore it is energetically favorable. Hence these antiphase domain walls which are observed in Nd-doped LSCO around $1/8$ of filling [13] seem also to be a rather common feature of the theoretically investigated stripe structures. As a consequence, in our charge-spin structure, the spin order follows the relation $\Delta^{spin}(\mathbf{R}) \sim \cos[q_c(x + y)/2] \cos[q_c(x - y)/2] \sim \cos(\mathbf{q}_s^+ \mathbf{R}) + \cos(\mathbf{q}_s^- \mathbf{R})$ where the spin scattering

vectors are given by $\mathbf{q}_s^+ = q_c(1, 0)$ and $\mathbf{q}_s^- = q_c(0, 1)$ respectively. Thus this kind of two-dimensional scattering displays a deviation between charge- and spin direction of 45° where the latter is compatible with the results of neutron scattering experiments [14,15]. Only in case of a LTT distortion both charge- and spin scattering collapse into a single direction leading to a reduction of T_c [13].

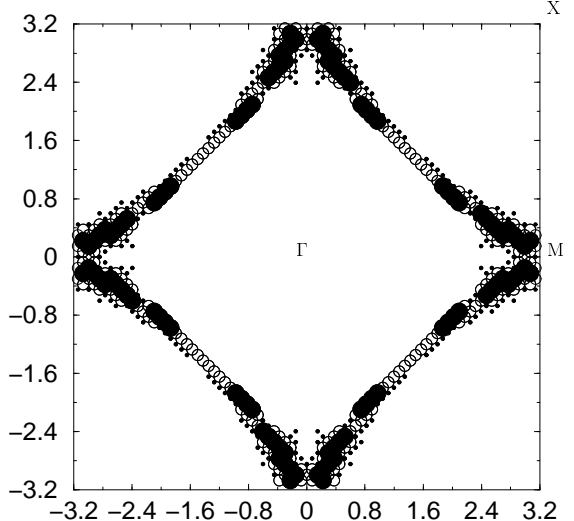


FIG. 3. Fermi surface for a system with two-dimensional diagonal CDW modulation ($q_c = \pi/5, \lambda = 0.01$). The plot is for temperature $T = 100K$. The spectral weight has been integrated over an energy window of 30meV around E_F . Intensities: $I > 50\%$: full points, $10\% < I < 50\%$: circles, $1\% < I < 10\%$: small dots.

As in the case of Bi2212 we restrict in the following on the charge channel and as discussed above we consider scattering along the $\mathbf{q}_c^\pm = (1, \pm 1)$ directions. To gain some qualitative insight we consider first the static non-superconducting case inspired by the approach described in Ref. [25] where we have derived an effective interaction $\frac{1}{2N} \sum_q V_q \rho_q \rho_{-q}$ for charge carriers close to an incommensurate CDW instability. Upon factorizing the interaction the two-dimensional eggbox-type charge modulation can be implemented by $\langle \rho_q \rangle^{egg} = \langle \rho_q \rangle [\delta_{q, q_c^+} + \delta_{q, q_c^-}]$ which in the static limit identifies the coupling parameter λ with the order parameter of the CDW $V(\mathbf{q}_c) \langle \rho_{\mathbf{q}_c} \rangle$. The resulting one particle hamiltonian can now be diagonalized and as a result we show in Fig. 3 the Fermi surface for an eggbox-type charge modulation with scattering vectors $\mathbf{q}_c = \pi/5(1, \pm 1)$.

Obviously diagonal CDW scattering strongly reduces the spectral intensity of the Fermi surface along the $\Gamma \rightarrow X$ direction. This is connected with the fact that along the diagonals the scattering vector is parallel to the contours of the bare bandstructure. As a consequence the CDW scattering is most efficient in these regions since \mathbf{q}_c can connect states with equal energies leading to a redistribution of spectral weight near $(\pi/2, \pi/2)$.

Note that since the band disperses rather rapidly along $\Gamma \rightarrow X$ the vertical scattering we have adopted in case of Bi2212 would leave the electronic structure in this direction nearly unchanged and would not reproduce the experimental suppression of spectral weight along the $\Gamma \rightarrow X$ direction [21–23].

Quite obviously our simplified approach, where the spin degrees of freedom are neglected, cannot provide a quantitative description of the Fermi surface. However, we notice that a model based on spin degrees of freedom only, constrained by the neutron experiments to have hot spots near the M points could hardly account for the suppression of spectral weight along the $\Gamma \rightarrow X$ direction.

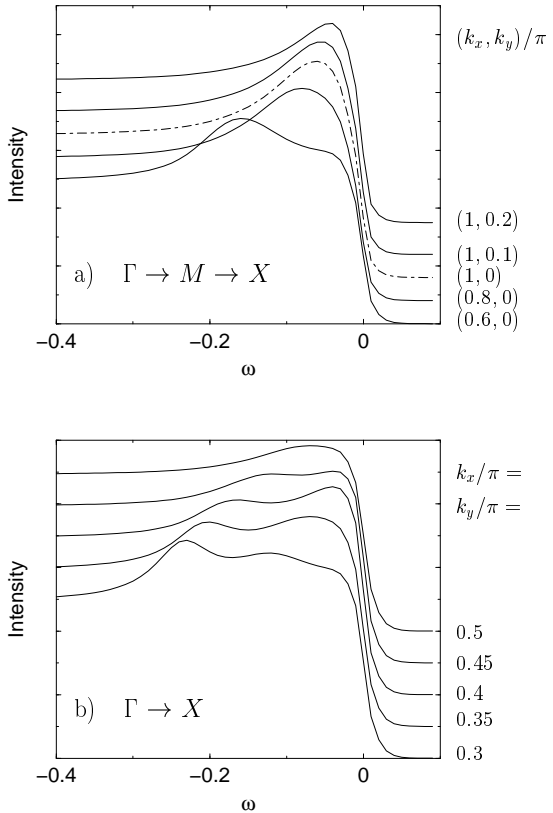


FIG. 4. Photoemission spectra for diagonal two-dimensional CDW scattering. As in the case of Bi2212 we have added a step-like function in order to model the background contribution. Parameter: $\omega_0 = 30\text{meV}$, $\Gamma = 0.01$, $\mathbf{q}_c = \pi/5(1, \pm 1)$.

Let us now extend the photoemission lineshape analysis to the superconducting state including dynamic incommensurate CDW scattering. We have found that for the LSCO compound a linear frequency distribution $g(\nu) = \frac{2\nu}{\omega_0^2} \Theta(\omega_0 - \nu)$ up to a cutoff energy ω_0 is more appropriate consistent with the experimental observation of low energy magnetic fluctuations in this compound. Fig. 4 shows selected energy distribution curves along $\Gamma \rightarrow M \rightarrow X$ (Fig. 4a) and $\Gamma \rightarrow X$ (Fig. 4b).

In the $(0, 0) \rightarrow (\pi, \pi)$ direction (Fig. 4b) one observes

only a broad and weak incoherent feature which disappears beyond $k_x = k_y \sim 0.45\pi$ corresponding to the FS crossing of the underlying bare bandstructure. In contrast the spectra around $(\pi, 0)$ (Fig. 4a) are composed of an also broadened but still well pronounced quasiparticle peak. Due to the small cutoff energy ω_0 in comparison with Bi2212 and the additional linear frequency distribution the hump feature is no longer separated from the sharp peak but both collapse into the broadened peak shown in Fig. 4b. Note that we were forced to use a rather large charge-charge correlation length (~ 100 lattice constants) in order to effectively suppress the quasiparticle peak along $(0, 0) \rightarrow (\pi, \pi)$. This finding needs to be commented. On the one hand it is surely conceivable that the poor quality of the surface in 214 materials is responsible for the width of the photoemission peaks. In this case this would be a spurious effect as far as the bulk electronic properties are concerned and our need of a large charge-charge correlation length would be fictitious. On the other hand the authors of Refs. [21–23] claim that a careful attention was paid to the surface treatment. Moreover, recent photoemission experiments [37] on overdoped LSCO have revealed a sharp spectral feature along the diagonal direction that is comparable to that of Bi2212. From this one would not expect strong disorder effects in the underdoped samples which should improve with decreasing Sr content. In this regard our finding of a large charge-charge correlation length could be taken seriously at least from a qualitative point of view. The presence of rather long-ranged charge-ordering correlations would rather naturally correspond to the much more visible presence of stripe correlations in 214 materials. Indeed, but for some inelastic neutron scattering [16] and some NMR/NQR [18,19] experiments in YBCO, the evidence for stripes is rather clear in 214 materials only, while it remains more elusive in the other classes of cuprates.

IV. CONCLUSION

We have demonstrated that the coupling of a superconducting system to dynamical incommensurate CDW fluctuations can account for the observed ARPES photoemission lineshapes in both Bi2212 and LSCO materials. According to our analysis the vertically oriented CDW fluctuations in Bi2212 are rather fast and short ranged leading to the experimentally observed dip-hump structure around the M-points whereas the lineshape along the diagonals is hardly affected by the scattering.

We emphasize again here that our analysis shares many similarities (both in the technical framework and in the results) with the one carried out in Ref. [26] (the renormalization function $Z(\omega)$ obtained from our approach is quasi identical to Fig. 1 in Ref. [26]). Therefore our work is not in contrast with Ref. [26] but rather comple-

mentar since the stripe fluctuations we consider here are anharmonic CDW's with the strong correlation playing a relevant role in the hole-poor regions, where antiferromagnetism is quite pronounced. For the sake of simplicity we only investigated the charge sector of the fluctuations. Nevertheless, the effects of spin [26] and charge (this work) fluctuations are similar indicating that these fluctuations may easily coexist and that there is no competition but rather cooperation between the two sectors. Of course a long way is still to be followed in order to integrate the two approaches by formalizing the interplay between charge and spin degrees of freedom. In particular an open relevant issue is to establish how the critical properties related to the charge instability are mirrored in the spin criticality. This intriguing but difficult issue is definitely beyond the present scope.

In case of LSCO the photoemission data can be described by a two-dimensional, diagonally oriented CDW which is slowly fluctuating and characterized by a rather large correlation length. This is consistent with the idea of long-range AF order coexisting with superconductivity in the 214 systems and also with the more pronounced tendency to form static charge textures in these materials. We have shown that within this scenario the QP along the $(0, 0) \rightarrow (\pi, \pi)$ direction can be effectively suppressed whereas around the M-points a broad quasiparticle peak persists. Finally we want to emphasize that since Δ_{SC} enters the calculation as an input parameter, our model does not include the phase fluctuations of the particle-particle pairs. These fluctuations should play a major role in destroying the quasiparticle peak above T_c [38]. However, the measurements in Refs. [21–23] on LSCO were done at rather low temperatures ($T=15\text{K}$) where such phase fluctuations are ineffective justifying our simplified model for the photoemission spectra.

At the present stage of the research in the field of superconducting cuprates our simplified analysis is particularly urgent since it illustrates that charge fluctuations can generically be quite effective sources of scattering between the quasiparticles providing spectral features which are not in contrast with experiments both in LSCO systems, where there seem to be little doubt that (dynamical) stripes are present, and in Bi2212 compounds, where no stringent evidence for stripe fluctuations is available. In this regard we show that different kinds of charge fluctuations can operate in different materials. Moreover, in the present situation, where even the experimental situation is rapidly evolving, we believe that our results can be useful in keeping the community flexible enough to effectively determine the intricate physical mechanisms of the superconducting cuprates.

ACKNOWLEDGMENTS

We would like to thank J. Mesot for providing the experimental data in Fig. 1. We also greatfully acknowledge useful discussions with S. Caprara, C. Castellani and C. Di Castro.

- [1] For a summary of this evidences see, e.g., the Introduction of C. Castellani, C. Di Castro, and M. Grilli, *Z. für Physik*, **103**, 137 (1997); J. L. Tallon, J. W. Loram, G. V. M. Williams, J. R. Cooper, I. R. Fisher, J. D. Johnson, M. P. Staines, C. Bernhard, *Phys. Stat. Sol. B* **215**, 531 (1999); J. L. Tallon, G. V. M. Williams, and J. W. Loram, *Physica C* **338**, 9 (2000).
- [2] G. S. Boebinger, Yoichi Ando, A. Passner, T. Kimura, M. Okuya, J. Shimoyama, K. Kishio, K. Tamasaku, N. Ichikawa, S. Uchida, *Phys. Rev. Lett.* **77**, 5417 (1996).
- [3] C. M. Varma, *Phys. Rev. Lett.* **75**, 898 (1995); C. M. Varma, *Phys. Rev. B* **55**, 14554 (1997) and references therein; F. Onufrieva and P. Pfeuty, *Phys. Rev. B* **61**, 799 (2000) and references therein; M. Vojta, Ying Zhang, and S. Sachdev, *Phys. Rev. B* **62**, 6721 (2000); T. Senthil and M. P. A. Fischer, *Phys. Rev. B* **62**, 7850 (2000); S. Chakravarty, *et al.*, cond-mat/0005443.
- [4] S. Sachdev and J. Ye, *Phys. Rev. Lett.* **69**, 2411 (1992).
- [5] V. Barzykin and D. Pines, *Phys. Rev. B* **52**, 13585 (1995) and references therein.
- [6] C. Castellani, C. Di Castro, and M. Grilli, *Phys. Rev. Lett.* **75**, 4650 (1995).
- [7] A. Perali, C. Castellani, C. Di Castro, and M. Grilli, *Phys. Rev. B* **54**, 16216 (1996).
- [8] C. Castellani, C. Di Castro, and M. Grilli, *J. Phys. Chem. Solids* **59**, 1694 (1998).
- [9] M. R. Norman and H. Ding, *Phys. Rev. B* **57**, R11089 (1998).
- [10] M. R. Norman, H. Ding, J. C. Campuzano, T. Takeuchi, M. Randeria, T. Yokoya, T. Takahashi, T. Mochiku, and K. Kadowaki, *Phys. Rev. Lett.* **79**, 3506 (1997).
- [11] For a recent review see, e.g., P. Bourges, cond-mat/0009373.
- [12] J. C. Campuzano, H. Ding, M. R. Norman, H. M. Fretwell, M. Randeria, A. Kaminski, J. Mesot, T. Takeuchi, T. Sato, T. Yokoya, T. Takahashi, T. Mochiku, K. Kadowaki, P. Guptasarma, D. G. Hinks, Z. Konstantinovic, Z. Z. Li, and H. Raffy, *Phys. Rev. Lett.* **83**, 3709 (1999).
- [13] J. M. Tranquada, B. J. Sternlieb, J. D. Axe, Y. Nakamura, and S. Uchida, *Nature* **375**, 561 (1995).
- [14] K. Yamada, C. H. Lee, K. Kurahashi, J. Wada, S. Wakimoto, S. Ueki, H. Kimura, Y. Endoh, S. Hosoya, G. Shirane, R. J. Birgeneau, M. Greven, M. A. Kastner, and Y. J. Kim, *Phys. Rev. B* **57**, 6165 (1998).
- [15] M. Arai, T. Nishijima, Y. Endoh, T. Egami, S. Tajima, K. Tomimoto, Y. Shiohara, M. Takahashi, A. Garrett, S. Bennington, *Phys. Rev. Lett.* **83**, 608 (1999).

- [16] H. A. Mook and F. Doğan, *Nature* **401**, 145 (1999).
- [17] G. B. Teitelbaum, B. Büchner, H. de Gronckel, *cond-mat/0005090*.
- [18] A. Suter, M. Mali, J. Roos, D. Brinkmann, J. Karpinski, and E. Kaldis, *Phys. Rev. B* **56**, 5542 (1997); I. Eremin, M. Eremin, S. Varlamov, D. Brinkmann, M. Mali, and J. Roos, *Phys. Rev. B* **56**, 11305 (1997).
- [19] S. Krämer, M. Mehring, *Phys. Rev. Lett.* **83**, 396 (1999).
- [20] A. W. Hunt, P. M. Singer, K. R. Thurber, and T. Imai, *Phys. Rev. Lett.* **82**, 4300 (1999).
- [21] A. Ino, C. Kim, M. Nakamura, T. Yoshida, T. Mizokawa, Z.-X. Shen, A. Fujimori, T. Kakeshita, H. Eisaki, and S. Uchida, *Phys. Rev. B* **62**, 4137 (2000).
- [22] A. Ino, C. Kim, M. Nakamura, T. Yoshida, T. Mizokawa, Z.-X. Shen, A. Fujimori, T. Kakeshita, H. Eisaki, and S. Uchida, *cond-mat/0005370*.
- [23] X. J. Zhou, T. Yoshida, S. A. Kellar, P. V. Bognaov, E. D. Lu, A. Lanzara, M. Nakamura, T. Noda, T. Kakeshita, H. Eisaki, S. Uchida, A. Fujimori, Z. Hussain, Z.-X. Shen, *cond-mat/0009002*.
- [24] T. Tohyama, S. Nagai, Y. Shibata, and S. Maekawa, *Phys. Rev. Lett.* **82**, 4910 (1999).
- [25] G. Seibold, F. Becca, F. Bucci, C. Castellani, C. Di Castro, and M. Grilli, *Europ. Phys. J. B* **13**, 87 (2000).
- [26] M. Eschrig and M. R. Norman, *Phys. Rev. Lett.* **85**, 3261 (2000).
- [27] A. P. Kampf and J. R. Schrieffer, *Phys. Rev. B* **42**, 7967 (1990).
- [28] M. R. Norman, *Phys. Rev. B* **61**, 16117 (2000).
- [29] C. Kim, P. J. White, Z.-X. Shen, T. Tohyama, Y. Shibata, S. Maekawa, B. O. Wells, Y. J. Kim, R. J. Birgeneau, and M. A. Kastner, *Phys. Rev. Lett.* **B 80**, 4245 (1998).
- [30] S. Engelsberg and J. R. Schrieffer, *Phys. Rev.* **131**, 993 (1963).
- [31] A. Kaminski, M. Randeria, J. C. Campuzano, M. R. Norman, H. Fretwell, J. Mesot, T. Sato, T. Takahashi, K. Kadowaki, *cond-mat/0004482*.
- [32] T. Valla, A. V. Fedorov, P. D. Johnson, B. O. Wells, S. L. Hulbert, Q. Li, G. D. Gu, N. Koshizuka, *Science* **258**, 2110 (1999).
- [33] L. Taillefer, B. Lussier, R. Gagnon, K. Behnia, and H. Aubin, *Phys. Rev. Lett.* **79**, 483 (1997); M. Chiao, R. W. Hill, C. Lupien, L. Taillefer, P. Lambert, R. Gagnon, P. Fournier, *Phys. Rev. B* **62**, 3554 (2000).
- [34] J. M. Tranquada, *Physica B* **241-243**, (1998).
- [35] Y. S. Lee, R. J. Birgeneau, M. A. Kastner, Y. Endoh, S. Wakimoto, K. Yamada, R. W. Erwin, S.-H. Lee, and G. Shirane, *Phys. Rev. B* **60**, 3643 (1999).
- [36] H. Kimura, H. Matsushita, K. Hirota, Y. Endoh, K. Yamada, G. Shirane, Y. S. Lee, M. A. Kastner, and R. J. Birgeneau, *Phys. Rev. B* **61**, 14366 (2000).
- [37] T. Yoshida, X. J. Zhou, M. Nakamura, S. A. Kellar, P. V. Bogdanov, E. D. Lu, A. Lanzara, Z. Hussain, A. Ino, T. Mizokawa, A. Fujimori, H. Eisaki, C. Kim, Z.-X. Shen, T. Kakeshita, S. Uchida, *cond-mat/0011172*.
- [38] M. Franz and A. J. Millis, *Phys. Rev. B* **58**, 14572 (1998).